Adaptive Backstepping Attitude Control of a Rigid Body with State Quantization

Siri Marte Schlanbusch[1], Jing Zhou[1] and Rune Schlanbusch[2]

[1]Department of Engineering Sciences
University of Agder
4879 Grimstad, Norway

[2]Norwegian Research Centre AS
4879 Grimstad, Norway

Abstract

In this paper, the attitude tracking control problem of a rigid body is investigated where the states are quantized. An adaptive backstepping based control scheme is developed and a new approach to stability analysis is developed by constructing a new compensation scheme for the effects of the vector state quantization. It is shown that all closed-loop signals are ensured uniformly bounded and the tracking errors converge to a compact set containing the origin. Experiments on a 2 degrees-of-freedom helicopter system illustrate the proposed control scheme.

B.1 Introduction

The interest for quantized control has attracted considerable attention in recent years due to its theoretical and practical importance in practical engineering, where signals are required to be quantized and transmitted via a common communication network. An important aspect is to use quantization schemes that yield sufficient precision, but reduce the communication burden over the network.

A great number of representative results have been reported on analysis and control of feedback systems with input quantization, as can be observed in [1–7]. The feedback control problem of systems with state quantization has been studied in [8–11], where the system dynamics in these works are precisely known. As we know, system uncertainties and non-linearity inevitably exist in physical systems. Only a few work using an adaptive approach have been reported to solve the state quantization problem for uncertain linear systems in [12] and uncertain nonlinear systems in [13].

Quantized control of rigid bodies is a potential problem. For example, the remote

control of a group of UAVs or robots, where the signals are transmitted over a shared network with limited communication information. Attitude stabilization with input quantization was investigated in [14] using a fixed-time sliding mode control. Trajectory tracking control for autonomous underwater vehicles with the effect of quantization was investigated in [15] using a sliding mode controller, where the considered systems are completely known. In [16], adaptive tracking control was proposed for underactuated autonomous underwater vehicles with input quantization. Uncertainties and non-linearities always exist in many practical systems. Thus it is more reasonable to consider controller design for uncertain nonlinear systems.

Adaptive backstepping technique was proposed in the 1990's in [17] to deal with plant non-linearity and parameter uncertainties. Several results have been reported on adaptive backstepping control with input quantization, e.g in [6, 7, 18, 19] for uncertain nonlinear systems, in [20] for a 2-DOF helicopter system, in [16] for tracking control for under-actuated autonomous underwater vehicles and in [21] for formation tracking control for a group of UAVs. However, adaptive backstepping control results to address uncertain systems with state quantization are very limited. One major difficulty to deal with the state quantization is that the backstepping technique requires differentiating virtual controls and in turn the states by applying chain rule. If the states are quantized, they become discontinuous and therefore it is difficult to analyze the resulting control system with the current backstepping based approaches. This problem was solved in [13] where the states were quantized by a static bounded quantizer.

This paper is concerned with the attitude tracking control of uncertain nonlinear rigid body systems with state quantization. A new backstepping based adaptive controller and a new approach to stability analysis are proposed. Compared to [13] for single-input-single-output (SISO) systems, this paper considers multiple-input-multiple-output (MIMO) uncertain systems with state quantization. A uniform quantization is included when tested on a 2 degrees-of-freedom (DOF) helicopter system from Quanser, with challenges in controller design due to the nonlinear behavior, the cross coupling effect between inputs and outputs, and with uncertainties both in the model and the parameters. It is analytically shown how the choice of quantization level affects the tracking performance, where a higher quantization level increases the tracking error. The experiments on the helicopter system illustrate the proposed scheme.

B.2 Dynamical Model and Problem Formulation

B.2.1 Notations

The symbol $\boldsymbol{\omega}_{b,a}^{c}$ denotes angular velocity of frame a relative to frame b, expressed in frame c; $\boldsymbol{R}_{a}^{b}$ is the rotation matrix from frame a to frame b; the cross product operator $\times$ between two vectors $\boldsymbol{a}$ and $\boldsymbol{b}$ is written as $\boldsymbol{S}(\boldsymbol{a})\boldsymbol{b}$ where $\boldsymbol{S}$ is skew-symmetric; $\lambda_{\max}(\cdot)$ and $\lambda_{\min}(\cdot)$ denotes the maximum and minimum eigenvalue of the matrix $(\cdot)$, and $\|\cdot\|$ denotes the $\mathcal{L}_2$-norm and induced $\mathcal{L}_2$-norm for vectors and matrices, respectively.

B.2.2 Attitude Dynamics

The orientation of a rigid body in frame b, relative to an inertial frame i, can be described by a unit quaternion, $\boldsymbol{q} = [\eta, \varepsilon_1, \varepsilon_2, \varepsilon_3]^\top = [\eta, \boldsymbol{\varepsilon}^\top]^\top \in \mathbb{S}^3 = \{x \in \mathbb{R}^4 : \boldsymbol{x}^\top \boldsymbol{x} = 1\}$ that is a complex number, where $\eta = \cos(\upsilon/2) \in \mathbb{R}$ is the real part and $\boldsymbol{\varepsilon} = \boldsymbol{k}\sin(\upsilon/2) \in \mathbb{R}^3$ is the imaginary part, where υ is the Euler angle and $\boldsymbol{k}$ is the Euler axis, and $\mathbb{S}^3$ is the non-Euclidean three-sphere. We consider a fully actuated rigid body with equations of motion for the attitude dynamics defined as

$$\dot{\boldsymbol{q}} = \boldsymbol{T}(\boldsymbol{q})\boldsymbol{\omega}, \tag{B.1}$$

$$\boldsymbol{J}\dot{\boldsymbol{\omega}} = \boldsymbol{\Psi}(\boldsymbol{q}, \boldsymbol{\omega}) + \boldsymbol{\Phi}(\boldsymbol{\omega})\boldsymbol{\theta} + \boldsymbol{B}\boldsymbol{u}, \tag{B.2}$$

with $\boldsymbol{\omega}_{i,b}^{b} = \boldsymbol{\omega} \in \mathbb{R}^3$, and where

$$\boldsymbol{T}(\boldsymbol{q}) = \frac{1}{2}\begin{bmatrix} -\boldsymbol{\varepsilon}^\top \\ \eta\boldsymbol{I} + \boldsymbol{S}(\boldsymbol{\varepsilon}) \end{bmatrix} \in \mathbb{R}^{4\times 3}, \tag{B.3}$$

$\boldsymbol{J} = \mathrm{diag}(J_x, J_y, J_z) \in \mathbb{R}^{3\times 3}$ is the inertia matrix about the origin o, and is positive definite,

$$\boldsymbol{\Psi} = -\boldsymbol{S}(\boldsymbol{\omega})(\boldsymbol{J}\boldsymbol{\omega}) - \boldsymbol{g}(\boldsymbol{q}) \ \in \mathbb{R}^3, \tag{B.4}$$

$$\boldsymbol{\Phi} = \mathrm{diag}(-\boldsymbol{\omega}) \ \in \mathbb{R}^{3\times 3}, \tag{B.5}$$

are known nonlinear functions of $\boldsymbol{q}$ and $\boldsymbol{\omega}$, the vector $\boldsymbol{\theta} \in \mathbb{R}^3$ is unknown and constant, the control allocation matrix $\boldsymbol{B} \in \mathbb{R}^{3\times 3}$ and the control input $\boldsymbol{u} \in \mathbb{R}^3$. The matrix $\boldsymbol{I}$ denotes the identity matrix and $\boldsymbol{S}(\cdot)$ is the skew-symmetric matrix given by

$$\boldsymbol{S}(\boldsymbol{\varepsilon}) = \begin{bmatrix} 0 & -\varepsilon_3 & \varepsilon_2 \\ \varepsilon_3 & 0 & -\varepsilon_1 \\ -\varepsilon_2 & \varepsilon_1 & 0 \end{bmatrix}. \tag{B.6}$$

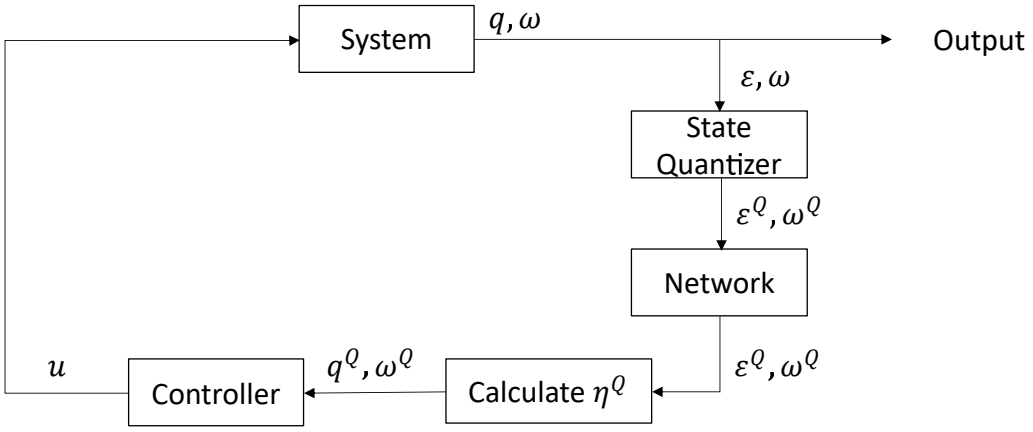

Figure B.1: Control system with state quantization over a network.

The moment caused by the gravitational force is

$$\boldsymbol{g}(\boldsymbol{q}) = -\boldsymbol{S}(\boldsymbol{r}_g^b)\boldsymbol{R}_i^b \boldsymbol{f}_g^i \in \mathbb{R}^3, \tag{B.7}$$

where $\boldsymbol{r}_g^b = [x_g \ y_g \ z_g]^\top$ is the distance from the origin to the center of mass, $\boldsymbol{f}_g^i = [0 \ \ 0 \ \ -mg]^\top$, m is the mass of the rigid body, and g is the gravity acceleration. If $\boldsymbol{r}_g^b = \boldsymbol{0} \implies \boldsymbol{g(q)} = 0$ and the rotation is about center of mass.

The orientation between two frames can be described by a rotation matrix given as

$$\boldsymbol{R}(\boldsymbol{q}) = \boldsymbol{I} + 2\eta \boldsymbol{S}(\boldsymbol{\varepsilon}) + 2\boldsymbol{S}^2(\boldsymbol{\varepsilon}), \tag{B.8}$$

where $\boldsymbol{R} \in SO(3)$ that is a special orthogonal group of order 3, and has the property

$$SO(3) = \{\boldsymbol{R} \in \mathbb{R}^{3\times 3} : \boldsymbol{R}^\top \boldsymbol{R} = \boldsymbol{I}, \det(\boldsymbol{R}) = 1\}. \tag{B.9}$$

The time derivative of a rotation matrix can be expressed as

$$\dot{\boldsymbol{R}}_b^a = \boldsymbol{R}_b^a \boldsymbol{S}(\boldsymbol{\omega}_{a,b}^b) = \boldsymbol{S}(\boldsymbol{\omega}_{a,b}^a)\boldsymbol{R}_b^a. \tag{B.10}$$

Attitude and angular velocities are assumed to be measurable after quantization, and for the control allocation matrix it is assumed that $\det(\boldsymbol{B}) \neq 0$, i.e. the matrix is invertible.

B.2.3 Problem Statement

We consider a control system as shown in Fig. B.1, where the states $\boldsymbol{\varepsilon}, \boldsymbol{\omega}$ are quantized at the encoder side to be sent over a network. The network is assumed noiseless, so that the quantized state signal is recovered and sent to the controller. Only the

quantized states $\boldsymbol{\varepsilon}^Q, \boldsymbol{\omega}^Q$ are measured, and the quantized value of η is calculated as

$$\eta^Q = \pm\sqrt{1 - \boldsymbol{\varepsilon}^{Q\top}\boldsymbol{\varepsilon}^Q}, \tag{B.11}$$

to ensure that the property of unit quaternion, $\boldsymbol{q}^{Q\top}\boldsymbol{q}^Q = 1$, is fulfilled, where the quantized attitude is given by $\boldsymbol{q}^Q = [\eta^Q, \boldsymbol{\varepsilon}^{Q\top}]^\top$.

Remark 1. *The quantized value, η^Q, can be calculated based on the value of $\boldsymbol{\varepsilon}^Q$ and knowledge of the sign of $\eta(t_0)$ and the assumption of sign continuity of $\eta(t)$ based on derivative. We can do the calculation after the network communication, saving bandwidth by sending less data over the network.*

Remark 2. *If we are close to, or at $\eta = 0$, we might end up with $\boldsymbol{\varepsilon}^{Q\top}\boldsymbol{\varepsilon}^Q > 1$, and a scaling is needed to ensure we have a unit quaternion.*

Let $\boldsymbol{q}_{i,d} = \boldsymbol{q}_d$, $\boldsymbol{\omega}^i_{i,d} = \boldsymbol{\omega}_d$ be the desired attitude and angular velocity. The control objective is to design a control law for $\boldsymbol{u}(t)$ by utilizing only quantized states $\boldsymbol{q}^Q(t), \boldsymbol{\omega}^Q(t)$ to ensure that $\boldsymbol{q}^Q(t) \to \boldsymbol{q}_d(t)$ and $\boldsymbol{\omega}^Q(t) \to \boldsymbol{\omega}^Q_{i,d}(t)$ as $t \to \infty$, where the kinematic equation

$$\dot{\boldsymbol{q}}_d = \boldsymbol{T}(\boldsymbol{q}_d)\boldsymbol{\omega}^d_{i,d} = \frac{1}{2}\begin{bmatrix} -\boldsymbol{\varepsilon}_d^\top \\ \eta_d\boldsymbol{I} - \boldsymbol{S}(\boldsymbol{\varepsilon}_d) \end{bmatrix}\boldsymbol{\omega}_d, \tag{B.12}$$

is satisfied, and where all the signals in the closed-loop system are uniformly bounded. To achieve the objective, the following assumptions are imposed.

Assumption 1. *The functions $\boldsymbol{q}_d(t)$, $\boldsymbol{\omega}_d(t)$ and $\dot{\boldsymbol{\omega}}_d(t)$ are known, piecewise continuous and bounded, where $\|\boldsymbol{\omega}_d(t)\| < k_{\omega_d}$ and $\|\dot{\boldsymbol{\omega}}_d(t)\| < k_{\dot{\omega}_d}$ $\forall t \geq t_0$ where $k_{\omega_d}, k_{\dot{\omega}_d} > 0$.*

Assumption 2. *The unknown parameter vector $\boldsymbol{\theta}$ is bounded by $\|\boldsymbol{\theta}\| \leq k_\theta$, where k_θ is a positive constant. Also $\boldsymbol{\theta} \in C_\theta$, where C_θ is a known compact convex set.*

B.2.4 Quantizer

The quantizer considered in this paper has the following property

$$|x^Q - x| \leq \delta_x, \tag{B.13}$$

where x is a scalar signal and $\delta_x > 0$ denotes the quantization bound. A uniform quantizer is considered, which has intervals of fixed length and is defined as

$$x^Q = x_i \operatorname{sgn}(x), \quad x_i - \frac{l}{2} \leq |x| < x_i + \frac{l}{2}, \tag{B.14}$$

where $i = 0, 1, 2, ...$, $x_0 = 0$, $x_{i+1} = x_i + l$, $l > 0$ is the length of the quantization intervals and where $\text{sgn}(\cdot)$ is the signum function. Here $x^Q = x + d$, where d is the quantization error and is bounded by (B.13), where $\delta_x = l/2$. The uniform quantization $x^Q \in U = \{\pm x_i\}$.

B.3 Controller Design and Stability Analysis

In this section we will design adaptive feedback control laws for the rigid body using backstepping technique. We begin with a change of coordinates to the error variables, and first find the error variables when the states are not quantized. The tracking error $\boldsymbol{e}$, is given by the quaternion product

$$\boldsymbol{e} = \bar{\boldsymbol{q}}_{i,d} \otimes \boldsymbol{q}_{i,b} = \begin{bmatrix} \tilde{\eta} \\ \tilde{\boldsymbol{\varepsilon}} \end{bmatrix} = \begin{bmatrix} \eta_d \eta + \boldsymbol{\varepsilon}_d^\top \boldsymbol{\varepsilon} \\ \eta_d \boldsymbol{\varepsilon} - \eta \boldsymbol{\varepsilon}_d - S(\boldsymbol{\varepsilon}_d)\boldsymbol{\varepsilon} \end{bmatrix} \in \mathbb{S}^3, \tag{B.15}$$

where $\bar{\boldsymbol{q}} = [\eta \ \ -\boldsymbol{\varepsilon}^\top]^\top$ is the inverse rotation given by the complex conjugate. If $\boldsymbol{q}_{i,b} = \boldsymbol{q}_{i,d}$ then $\boldsymbol{e} = [\pm 1 \ \mathbf{0}^\top]^\top$. Because there exists two different equilibria using quaternion coordinates, global stability can not be achieved, even though $\boldsymbol{e}$ and $-\boldsymbol{e}$ represents the same physical attitude [22]. We include one further assumption as follows:

Assumption 3. $\text{sgn}(\tilde{\eta}(t_0)) = \text{sgn}(\tilde{\eta}(t)) \ \ \forall t \geq t_0$.

Remark 3. *Assumption 3 is imposed to avoid the problem when the attitude error is close to* $E \triangleq \{\boldsymbol{e} \in \mathbb{S}^3 \ : \ \tilde{\eta} = 0\}$*, where the solution is not robust when a disturbance/quantization is introduced.*

The relative error kinematics is

$$\dot{\boldsymbol{e}} = \boldsymbol{T}(\boldsymbol{e})\boldsymbol{\omega}_e, \tag{B.16}$$

where $\boldsymbol{T}(\cdot)$ is defined in (B.3), and the angular velocity error

$$\boldsymbol{\omega}_e = \boldsymbol{\omega} - \boldsymbol{R}_i^b \boldsymbol{\omega}_d. \tag{B.17}$$

Since we have two equilibrium points, we introduce the change of coordinates

$$\boldsymbol{z}_{1\pm} = \begin{bmatrix} 1 \mp \tilde{\eta} \\ \tilde{\boldsymbol{\varepsilon}} \end{bmatrix}, \quad \boldsymbol{z}_2 = \boldsymbol{\omega}_e - \boldsymbol{\alpha}, \tag{B.18}$$

$$\dot{\boldsymbol{z}}_{1\pm} = \frac{1}{2} \begin{bmatrix} \pm \tilde{\boldsymbol{\varepsilon}}^\top \\ (\tilde{\eta}\boldsymbol{I} + \boldsymbol{S}(\tilde{\boldsymbol{\varepsilon}})) \end{bmatrix} \boldsymbol{\omega}_e \triangleq \frac{1}{2} \boldsymbol{G}(\boldsymbol{e})^\top \boldsymbol{\omega}_e, \tag{B.19}$$

where $\boldsymbol{z}_{1+}$ is the equilibrium point when $\tilde{\eta}(t_0) \geq 0$ and $\boldsymbol{z}_{1-}$ is the equilibrium point when $\tilde{\eta}(t_0) < 0$, the matrix $\boldsymbol{G}^\top \in \mathbb{R}^{4\times 3}$, and where $\boldsymbol{\alpha}$ is a virtual controller chosen as

$$\boldsymbol{\alpha} = -\boldsymbol{C}_1 \boldsymbol{G} \boldsymbol{z}_1 \in \mathbb{R}^3, \tag{B.20}$$

where $\boldsymbol{C}_1 \in \mathbb{R}^{3\times 3}$ is a positive definite matrix.

Remark 4. *Without the change of coordinates to $\boldsymbol{z}_{1\pm}$ one might end up with an unwanted or less optimal rotation of the rigid body.*

By multiplication, it can be shown that $\boldsymbol{G}\boldsymbol{z}_1 = \pm\tilde{\boldsymbol{\varepsilon}}$, and then from (B.20) we have

$$\dot{\boldsymbol{\alpha}} = \mp\frac{1}{2}\boldsymbol{C}_1\left[\tilde{\eta}\boldsymbol{I} + \boldsymbol{S}(\tilde{\boldsymbol{\varepsilon}})\right]\boldsymbol{\omega}_e. \tag{B.21}$$

The angular velocity error and angular velocity are bounded

$$\begin{aligned}\|\boldsymbol{\omega}_e\| &\leq \|\boldsymbol{z}_2 + \boldsymbol{\alpha}\| \leq \|\boldsymbol{z}_2\| + \lambda_{\max}(\boldsymbol{C}_1)\|\boldsymbol{G}\|\|\boldsymbol{z}_1\| \leq [1 + \lambda_{\max}(\boldsymbol{C}_1)]\|\boldsymbol{z}\| \\ &\triangleq d_a\|\boldsymbol{z}\|, \end{aligned} \tag{B.22}$$

$$\begin{aligned}\|\boldsymbol{\omega}\| &\leq \|\boldsymbol{\omega}_e + \boldsymbol{R}_i^b\boldsymbol{\omega}_d\| \leq d_a\|\boldsymbol{z}\| + \|\boldsymbol{R}_i^b\|\|\boldsymbol{\omega}_d\| \\ &\leq d_a\|\boldsymbol{z}\| + k_{\omega_d}, \end{aligned} \tag{B.23}$$

where $\boldsymbol{z} = [\boldsymbol{z}_1^\top, \boldsymbol{z}_2^\top]^\top$. When the states are quantized, the quantization error of the quaternion can be expressed as

$$\boldsymbol{d}_q = \bar{\boldsymbol{q}}_{i,b} \otimes \boldsymbol{q}_{i,Q} = \begin{bmatrix} d_\eta \\ \boldsymbol{d}_\varepsilon \end{bmatrix} = \begin{bmatrix} \eta\eta^Q + \boldsymbol{\varepsilon}^\top\boldsymbol{\varepsilon}^Q \\ \eta\boldsymbol{\varepsilon}^Q - \eta^Q\boldsymbol{\varepsilon} - S(\boldsymbol{\varepsilon})\boldsymbol{\varepsilon}^Q \end{bmatrix}, \tag{B.24}$$

where $\boldsymbol{d}_\varepsilon$ is the quantization error and bounded by $\|\boldsymbol{d}_\varepsilon\| \leq k_\varepsilon\|\boldsymbol{\delta}_\varepsilon\|$ from (B.13) and where $k_\varepsilon > 1$ is a positive constant, and d_η is bounded from the unity property of unit quaternion. If $\boldsymbol{q}^Q = \boldsymbol{q}$ and there is no quantization error, $\boldsymbol{d}_q = [1\ 0\ 0\ 0]^\top$. The tracking error with the quantized value of the unit quaternion $\boldsymbol{e}^Q$, is given by

$$\boldsymbol{e}^Q = \bar{\boldsymbol{q}}_{i,d} \otimes \boldsymbol{q}_{i,Q} = \begin{bmatrix} \tilde{\eta}^Q \\ \tilde{\boldsymbol{\varepsilon}}^Q \end{bmatrix} = \begin{bmatrix} \eta_d\eta^Q + \boldsymbol{\varepsilon}_d^\top\boldsymbol{\varepsilon}^Q \\ \eta_d\boldsymbol{\varepsilon}^Q - \eta^Q\boldsymbol{\varepsilon}_d - S(\boldsymbol{\varepsilon}_d)\boldsymbol{\varepsilon}^Q \end{bmatrix}, \tag{B.25}$$

and can also be described by

$$\begin{aligned}\boldsymbol{e}^Q = \boldsymbol{q}_{d,b} \otimes \boldsymbol{q}_{b,Q} = \boldsymbol{e} \otimes \boldsymbol{d}_q &= \begin{bmatrix} \tilde{\eta}d_\eta - \tilde{\boldsymbol{\varepsilon}}^\top\boldsymbol{d}_\varepsilon \\ d_\eta\tilde{\boldsymbol{\varepsilon}} + \tilde{\eta}\boldsymbol{d}_\varepsilon + S(\tilde{\boldsymbol{\varepsilon}})\boldsymbol{d}_\varepsilon \end{bmatrix} \\ &= \begin{bmatrix} \tilde{\eta}^Q \\ \tilde{\boldsymbol{\varepsilon}} + (d_\eta - 1)\tilde{\boldsymbol{\varepsilon}} + \tilde{\eta}\boldsymbol{d}_\varepsilon + S(\tilde{\boldsymbol{\varepsilon}})\boldsymbol{d}_\varepsilon \end{bmatrix} \triangleq \begin{bmatrix} \tilde{\eta}^Q \\ \tilde{\boldsymbol{\varepsilon}} + \boldsymbol{d}_{\tilde{\varepsilon}} \end{bmatrix}, \end{aligned} \tag{B.26}$$

where the value of $\boldsymbol{d}_{\tilde{\varepsilon}}$ depends on the quantization error given in (B.24). If there is no quantization error, $\boldsymbol{d}_{\tilde{\varepsilon}} = \boldsymbol{0}$. The quantization of the angular velocities $\boldsymbol{\omega}$ can be expressed as

$$\boldsymbol{\omega}^Q = \boldsymbol{\omega} + \boldsymbol{d}_\omega, \tag{B.27}$$

where $\boldsymbol{d}_\omega$ is the quantization error and bounded by $\|\boldsymbol{d}_\omega\| \leq \|\boldsymbol{\delta}_\omega\|$ from (B.13). We choose the adaptive controller

$$\boldsymbol{u}(t) = \boldsymbol{B}^{-1}\Big[-\boldsymbol{G}^Q \boldsymbol{z}_1^Q - \boldsymbol{C}_2 \boldsymbol{z}_2^Q - \boldsymbol{\Phi}^Q \hat{\boldsymbol{\theta}} - \boldsymbol{\Psi}^Q - \boldsymbol{J}\Big(\boldsymbol{S}(\boldsymbol{\omega}^Q)\boldsymbol{R}_i^Q \boldsymbol{\omega}_d - \boldsymbol{R}_i^Q \dot{\boldsymbol{\omega}}_d - \bar{\boldsymbol{\alpha}}^Q\Big)\Big], \tag{B.28}$$

$$\dot{\hat{\boldsymbol{\theta}}} = \mathrm{Proj}\{\boldsymbol{\Gamma}\boldsymbol{\Phi}^Q \boldsymbol{z}_2^Q\}, \tag{B.29}$$

where $\hat{\boldsymbol{\theta}}$ is the estimated value of $\boldsymbol{\theta}$, the vector $\tilde{\boldsymbol{\theta}} = \boldsymbol{\theta} - \hat{\boldsymbol{\theta}}$, the matrices $\boldsymbol{C}_2,\ \boldsymbol{\Gamma} \in \mathbb{R}^{3\times 3}$ are positive definite, and where $\mathrm{Proj}\{\cdot\}$ is the projection operator given in [17], and

$$\boldsymbol{z}_{1\pm}^Q = \begin{bmatrix} 1 \mp \tilde{\eta}^Q \\ \tilde{\boldsymbol{\varepsilon}}^Q \end{bmatrix}, \tag{B.30}$$

$$\boldsymbol{z}_2^Q = \boldsymbol{\omega}_e^Q - \boldsymbol{\alpha}^Q, \tag{B.31}$$

$$\boldsymbol{G}(\boldsymbol{e}^Q)^\top = \begin{bmatrix} \pm\tilde{\boldsymbol{\varepsilon}}^{Q\top} \\ \tilde{\eta}^Q \boldsymbol{I} + \boldsymbol{S}(\tilde{\boldsymbol{\varepsilon}}^Q) \end{bmatrix}, \tag{B.32}$$

$$\boldsymbol{\alpha}^Q = -\boldsymbol{C}_1 \boldsymbol{G}^Q \boldsymbol{z}_1^Q = \mp \boldsymbol{C}_1 \tilde{\boldsymbol{\varepsilon}}^Q, \tag{B.33}$$

$$\boldsymbol{\Psi}^Q = -\boldsymbol{S}(\boldsymbol{\omega}^Q)(\boldsymbol{J}\boldsymbol{\omega}^Q) - \boldsymbol{g}(\boldsymbol{q}^Q), \tag{B.34}$$

$$\boldsymbol{\Phi}^Q = \mathrm{diag}(-\boldsymbol{\omega}^Q), \tag{B.35}$$

$$\boldsymbol{g}(\boldsymbol{q}^Q) = -\boldsymbol{S}(\boldsymbol{r}_g^b)\boldsymbol{R}_i^Q \boldsymbol{f}_g^i, \tag{B.36}$$

$$\bar{\boldsymbol{\alpha}}^Q \triangleq \mp\frac{1}{2}\boldsymbol{C}_1\Big[\tilde{\eta}^Q \boldsymbol{I} + \boldsymbol{S}(\tilde{\boldsymbol{\varepsilon}}^Q)\Big]\boldsymbol{\omega}_e^Q, \tag{B.37}$$

$$\boldsymbol{\omega}_e^Q = \boldsymbol{\omega}^Q - \boldsymbol{R}_i^Q \boldsymbol{\omega}_d, \tag{B.38}$$

$$\boldsymbol{R}_i^Q = \boldsymbol{R}_b^Q \boldsymbol{R}_i^b. \tag{B.39}$$

Remark 5. *The projection operator* $\mathrm{Proj}\{\cdot\}$ *in* (B.29) *ensures that the estimates and estimation errors are nonzero and within known bounds, that is* $\|\hat{\boldsymbol{\theta}}\| \leq k_\theta$ *and* $\|\tilde{\boldsymbol{\theta}}\| \leq k_\theta$*, and has the property* $-\tilde{\boldsymbol{\theta}}^\top \boldsymbol{\Gamma}^{-1}\mathrm{Proj}(\boldsymbol{\tau}) \leq -\tilde{\boldsymbol{\theta}}^\top \boldsymbol{\Gamma}^{-1}\boldsymbol{\tau}$*, which are helpful to guarantee the closed-loop stability.*

Remark 6. *Only the quantized states can be used in the designed controller. Since the quantized states are used in the design of the virtual controller* $\boldsymbol{\alpha}^Q$ *in* (B.33)*, the derivative of the virtual controller is discontinuous and can not be used in the design of the controller, as it is for the case when the states are not quantized. Instead we*

choose a function (B.37)*, that is designed as if the states are not quantized in* (B.21)*, where* $\partial\boldsymbol{\alpha}/\partial\tilde{\boldsymbol{\varepsilon}}$ *is used [13].*

We show the stability of the positive equilibrium point, i.e. $\boldsymbol{z}_1^Q = \boldsymbol{z}_{1+}^Q$. To ensure that all signals are bounded, we first establish some prelimenary results as stated in the following lemma.

Lemma 1. *The effects of state quantization are bounded by the following inequalities:*

$$\text{(i)}\ \boldsymbol{\omega}_e^Q = \boldsymbol{\omega} + \boldsymbol{d}_\omega - \boldsymbol{R}_b^Q \boldsymbol{R}_i^b \boldsymbol{\omega}_d \le \boldsymbol{\omega}_e + \Big(2k_\varepsilon\Big[\boldsymbol{S}(\boldsymbol{\delta}_\varepsilon)+\boldsymbol{S}^2(\boldsymbol{\delta}_\varepsilon)\Big]\boldsymbol{R}_i^b\boldsymbol{\omega}_d + \boldsymbol{\delta}_\omega\Big) \triangleq \boldsymbol{\omega}_e + \boldsymbol{\delta}_{\omega_e}, \tag{B.40}$$

$$\text{(ii)}\ \boldsymbol{z}_2^Q \le \boldsymbol{\omega}_e + \boldsymbol{\delta}_{\omega_e} + \boldsymbol{C}_1\tilde{\boldsymbol{\varepsilon}}^Q \le \boldsymbol{\omega}_e + \boldsymbol{\delta}_{\omega_e} - \boldsymbol{\alpha} + \boldsymbol{C}_1\boldsymbol{d}_{\tilde{\varepsilon}} \le \boldsymbol{z}_2 + (\boldsymbol{\delta}_{\omega_e} + \boldsymbol{C}_1 k_\varepsilon \boldsymbol{\delta}_\varepsilon) \triangleq \boldsymbol{z}_2 + \boldsymbol{\delta}_{z_2}, \tag{B.41}$$

$$\text{(iii)}\ \|\boldsymbol{G}\boldsymbol{z}_1 - \boldsymbol{G}^Q\boldsymbol{z}_1^Q\| = \|\tilde{\boldsymbol{\varepsilon}} - \tilde{\boldsymbol{\varepsilon}}^Q\| \le \|k_\varepsilon\boldsymbol{\delta}_\varepsilon\|, \tag{B.42}$$

$$\text{(iv)}\ \|\boldsymbol{R}_i^Q - \boldsymbol{R}_i^b\| \le \|-2d_\eta\boldsymbol{S}(\boldsymbol{d}_\varepsilon)+2\boldsymbol{S}^2(\boldsymbol{d}_\varepsilon)^\top\|\|\boldsymbol{R}_i^b\| \le 2\Big[k_\varepsilon\|\boldsymbol{\delta}_\varepsilon\| + k_\varepsilon^2\|\boldsymbol{\delta}_\varepsilon\|^2\Big] \triangleq d_R, \tag{B.43}$$

$$\text{(v)}\ \|\boldsymbol{\Psi} - \boldsymbol{\Psi}^Q\| \le \|-\boldsymbol{S}(\boldsymbol{\omega})(\boldsymbol{J}\boldsymbol{\omega})+\boldsymbol{S}(\boldsymbol{\omega}+\boldsymbol{d}_\omega)(\boldsymbol{J}(\boldsymbol{\omega}+\boldsymbol{d}_\omega))+\boldsymbol{S}(\boldsymbol{r}_g^b)\boldsymbol{R}_i^b\boldsymbol{f}_g^i - \boldsymbol{S}(\boldsymbol{r}_g^b)\boldsymbol{R}_i^Q\boldsymbol{f}_g^i\| \le \Big[\lambda_{\max}(\boldsymbol{J})\Big(\|\boldsymbol{\delta}_\omega\|^2 + 2k_{\omega_d}\|\boldsymbol{\delta}_\omega\|\Big) + \|\boldsymbol{r}_g^b\|d_R mg\Big] + \Big[2\lambda_{\max}(\boldsymbol{J})\|\boldsymbol{\delta}_\omega\|d_a\Big]\|\boldsymbol{z}\| \triangleq d_{\Psi_1} + d_{\Psi_2}\|\boldsymbol{z}\|, \tag{B.44}$$

$$\text{(vi)}\ \|\boldsymbol{S}(\boldsymbol{\omega})\boldsymbol{R}_i^b - \boldsymbol{S}(\boldsymbol{\omega}^Q)\boldsymbol{R}_i^Q\| \le \|-\boldsymbol{S}(\boldsymbol{\omega})[-2d_\eta\boldsymbol{S}(\boldsymbol{d}_\varepsilon) + 2\boldsymbol{S}^2(\boldsymbol{d}_\varepsilon)^\top]\boldsymbol{R}_i^b - \boldsymbol{S}(\boldsymbol{d}_\omega)\boldsymbol{R}_i^Q\| \le \|\boldsymbol{\omega}\|d_R + \|\boldsymbol{\delta}_\omega\| \le (k_{\omega_d}d_R + \|\boldsymbol{\delta}_\omega\|) + (d_a d_R)\|\boldsymbol{z}\| \triangleq d_{S_1} + d_{S_2}\|\boldsymbol{z}\|, \tag{B.45}$$

$$\text{(vii)}\ \|\bar{\boldsymbol{\alpha}}^Q - \dot{\boldsymbol{\alpha}}\| = \|\frac{1}{2}\boldsymbol{C}_1\Big[[\tilde{\eta}\boldsymbol{I} + \boldsymbol{S}(\tilde{\varepsilon})]\boldsymbol{\omega}_e - [\tilde{\eta}^Q\boldsymbol{I} + \boldsymbol{S}(\tilde{\varepsilon}^Q)]\boldsymbol{\omega}_e^Q\Big]\| \le \frac{1}{2}\lambda_{\max}(\boldsymbol{C}_1)\Big(2\|\boldsymbol{\omega}_e\| + \|\boldsymbol{\delta}_{\omega_e}\|\Big) \le \lambda_{\max}(\boldsymbol{C}_1)(\frac{1}{2}\|\boldsymbol{\delta}_{\omega_e}\| + d_a\|\boldsymbol{z}\|) \triangleq d_{\bar{\alpha}_1} + d_{\bar{\alpha}_2}\|\boldsymbol{z}\|. \tag{B.46}$$

Proof: The property of (B.40) follows from (B.38), with the use of (B.8), (B.24), (B.27) and (B.39). The property of (B.41) follows from (B.31), with the use of (B.40), (B.33), (B.26), (B.18) and (B.20). The definition in (B.26) is used for inequality (B.42). The property of (B.43) follows by using (B.39) and (B.24), together with the property of (B.8). Using (B.4), (B.7), (B.13), (B.23), (B.27), (B.34), (B.36) and (B.43) the bound in (B.44) is ensured. The property of (B.45) follows by using (B.23), (B.24), (B.27), (B.43), (B.39) together with the properties of (B.8) and (B.13). The property of (B.46) follows by using (B.21), (B.22), (B.37), (B.40) and the property of unit quaternion.

We state our main results based on the control scheme in the following theorem.

Theorem 1. *Considering the closed-loop adaptive system consisting of the plant* (B.1)-(B.2) *with state quantization satisfying the bounded property* (B.13)*, the adaptive controller* (B.28)*, the update law* (B.29) *and Assumptions 1-3. If the gain matrices* $\boldsymbol{C}_1$ *and* $\boldsymbol{C}_2$ *and quantization parameters* $\boldsymbol{\delta}_\varepsilon$ *and* $\boldsymbol{\delta}_\omega$ *are chosen to satisfy*

$$\frac{c_0}{2} - d_{V_1} \geq k > 0, \tag{B.47}$$

where c_0 *is the minimum eigenvalue of* $\boldsymbol{C}_0 = \min\{\boldsymbol{G}^\top \boldsymbol{C}_1 \boldsymbol{G}, \boldsymbol{C}_2\}$*,* k *is a positive constant, and* d_{V_1} *is defined as*

$$d_{V_1} = d_{\Psi_2} + d_{S_2}\lambda_{\max}(\boldsymbol{J})k_{\omega_d} + d_{\bar{\alpha}_2}\lambda_{\max}(\boldsymbol{J}), \tag{B.48}$$

all signals in the closed loop system are ensured to be uniformly bounded. The error signals will converge to a compact set, i.e.

$$\|\boldsymbol{z}(t)\| \leq \sqrt{\frac{a}{k}}, \tag{B.49}$$

where

$$\begin{aligned}
a &= d_{\theta_1} + \frac{1}{2c_0} d_{V_2}^2, && \text{(B.50)}\\
d_{\theta_1} &= k_\theta \|\boldsymbol{\delta}_\omega\| \|\boldsymbol{\delta}_{z_2}\| + k_\theta \|\boldsymbol{\delta}_{z_2}\| k_{\omega_d}, && \text{(B.51)}\\
d_{V_2} &= \lambda_{\max}(\boldsymbol{C}_2)\|\boldsymbol{\delta}_{z_2}\| + \|k_\varepsilon \boldsymbol{\delta}_\varepsilon\| + d_{\Psi_1} + d_{S_1}\lambda_{\max}(\boldsymbol{J})k_{\omega_d} + d_R\lambda_{\max}(\boldsymbol{J})k_{\dot{\omega}_d}\\
&\quad + d_{\bar{\alpha}_1}\lambda_{\max}(\boldsymbol{J}) + d_{\theta_2}, && \text{(B.52)}\\
d_{\theta_2} &= k_\theta \|\boldsymbol{\delta}_\omega\| + k_\theta d_a \|\boldsymbol{\delta}_{z_2}\|, && \text{(B.53)}
\end{aligned}$$

and is ultimately bounded. Tracking of a given reference signal is achieved, with a bounded error.

Proof: Considering the Lyapunov function

$$V(\boldsymbol{z}, \tilde{\boldsymbol{\theta}}, t) = \boldsymbol{z}_1^\top \boldsymbol{z}_1 + \frac{1}{2}\boldsymbol{z}_2^\top \boldsymbol{J}\boldsymbol{z}_2 + \frac{1}{2}\tilde{\boldsymbol{\theta}}^\top \boldsymbol{\Gamma}^{-1}\tilde{\boldsymbol{\theta}}, \tag{B.54}$$

then by following the controller design in (B.28)-(B.29), the derivative of (B.54) is given as

$$\begin{aligned}
\dot{V} &= \boldsymbol{z}_1^\top \boldsymbol{G}^\top \boldsymbol{z}_2 - \boldsymbol{z}_1^\top \boldsymbol{G}^\top \boldsymbol{C}_1 \boldsymbol{G}\boldsymbol{z}_1 + \boldsymbol{z}_2^\top \Big[\boldsymbol{\Phi}\boldsymbol{\theta} + \boldsymbol{\Psi} + \boldsymbol{B}\boldsymbol{u} + \boldsymbol{J}\Big(\boldsymbol{S}(\boldsymbol{\omega})\boldsymbol{R}_i^b \boldsymbol{\omega}_d - \boldsymbol{R}_i^b \dot{\boldsymbol{\omega}}_d - \dot{\boldsymbol{\alpha}}\Big)\Big]\\
&\quad - \tilde{\boldsymbol{\theta}}^\top \boldsymbol{\Gamma}^{-1}\dot{\hat{\boldsymbol{\theta}}}\\
&= -\boldsymbol{z}_1^\top \boldsymbol{G}^\top \boldsymbol{C}_1 \boldsymbol{G}\boldsymbol{z}_1 - \boldsymbol{z}_2^\top \boldsymbol{C}_2 \boldsymbol{z}_2^Q + \boldsymbol{z}_2^\top (\boldsymbol{G}\boldsymbol{z}_1 - \boldsymbol{G}^Q \boldsymbol{z}_1^Q) + \boldsymbol{z}_2^\top (\boldsymbol{\Psi} - \boldsymbol{\Psi}^Q)
\end{aligned}$$

$$+ \boldsymbol{z}_2^\top \boldsymbol{J}(\boldsymbol{S}(\boldsymbol{\omega})\boldsymbol{R}_i^b - \boldsymbol{S}(\boldsymbol{\omega}^Q)\boldsymbol{R}_i^Q)\boldsymbol{\omega}_d + \boldsymbol{z}_2^\top \boldsymbol{J}\Big(\boldsymbol{R}_i^Q - \boldsymbol{R}_i^b\Big)\dot{\boldsymbol{\omega}}_d + \boldsymbol{z}_2^\top \boldsymbol{J}(\bar{\boldsymbol{\alpha}}^Q - \dot{\boldsymbol{\alpha}})$$
$$+ \Big[\boldsymbol{z}_2^\top(\boldsymbol{\Phi}\boldsymbol{\theta} - \boldsymbol{\Phi}^Q\hat{\boldsymbol{\theta}}) - \tilde{\boldsymbol{\theta}}^\top\boldsymbol{\Phi}^Q\boldsymbol{z}_2^Q\Big]. \tag{B.55}$$

By using (B.5), (B.35), (B.29), (B.27), (B.41), (B.23) and Assumption 2 the last terms in (B.55) satisfy the inequality

$$\begin{aligned}\boldsymbol{z}_2^\top(\boldsymbol{\Phi}\boldsymbol{\theta}-\boldsymbol{\Phi}^Q\hat{\boldsymbol{\theta}})-\tilde{\boldsymbol{\theta}}^\top\boldsymbol{\Phi}^Q\boldsymbol{z}_2^Q &= \boldsymbol{\theta}^\top\boldsymbol{\Phi}\boldsymbol{z}_2 - \boldsymbol{\theta}^\top\boldsymbol{\Phi}^Q\boldsymbol{z}_2 + \tilde{\boldsymbol{\theta}}^\top\boldsymbol{\Phi}^Q\boldsymbol{z}_2 - \tilde{\boldsymbol{\theta}}^\top\boldsymbol{\Phi}^Q\boldsymbol{z}_2^Q \\ &\leq \|\boldsymbol{\theta}\|\|\boldsymbol{\Phi}-\boldsymbol{\Phi}^Q\|\|\boldsymbol{z}_2\| + \|\tilde{\boldsymbol{\theta}}\|\|\boldsymbol{\Phi}^Q\|\|\boldsymbol{z}_2-\boldsymbol{z}_2^Q\| \\ &\leq k_\theta\|\mathrm{diag}(-\boldsymbol{\omega})-\mathrm{diag}(-\boldsymbol{\omega}-\boldsymbol{d}_\omega)\|\|\boldsymbol{z}\|+k_\theta(\|\boldsymbol{\omega}\|+\|\boldsymbol{\delta}_\omega\|)\|\boldsymbol{\delta}_{z_2}\| \\ &\leq d_{\theta_1} + d_{\theta_2}\|\boldsymbol{z}\|. \end{aligned} \tag{B.56}$$

By using Young's inequality, the properties in Lemma 1, (B.56) and Assumption 1, the derivative of V in (B.55) can be obtained as

$$\begin{aligned}\dot{V} \leq & -\boldsymbol{z}_1^\top\boldsymbol{G}^\top\boldsymbol{C}_1\boldsymbol{G}\boldsymbol{z}_1 - \boldsymbol{z}_2^\top\boldsymbol{C}_2\boldsymbol{z}_2 + \lambda_{\max}(\boldsymbol{C}_2)\|\boldsymbol{\delta}_{z_2}\|\|\boldsymbol{z}\| + \|k_\varepsilon\boldsymbol{\delta}_\varepsilon\|\|\boldsymbol{z}\| + d_{\Psi_1}\|\boldsymbol{z}\| \\ & + d_{\Psi_2}\|\boldsymbol{z}\|^2 + d_{S_1}\lambda_{\max}(\boldsymbol{J})k_{\omega_d}\|\boldsymbol{z}\| + d_{S_2}\lambda_{\max}(\boldsymbol{J})k_{\omega_d}\|\boldsymbol{z}\|^2 + d_R\lambda_{\max}(\boldsymbol{J})k_{\dot{\omega}_d}\|\boldsymbol{z}\| \\ & + d_{\bar{\alpha}_1}\lambda_{\max}(\boldsymbol{J})\|\boldsymbol{z}\| + d_{\bar{\alpha}_2}\lambda_{\max}(\boldsymbol{J})\|\boldsymbol{z}\|^2 + d_{\theta_1} + d_{\theta_2}\|\boldsymbol{z}\| \\ \leq & -c_0\|\boldsymbol{z}\|^2 + d_{\theta_1} + d_{V_2}\|\boldsymbol{z}\| + d_{V_1}\|\boldsymbol{z}\|^2 \\ \leq & -(\frac{c_0}{2} - d_{V_1})\|\boldsymbol{z}\|^2 + d_{\theta_1} + \frac{1}{2c_0}d_{V_2}^2 \\ \leq & -k\|\boldsymbol{z}\|^2 + a < 0, \quad \forall\|\boldsymbol{z}\| > \sqrt{a/k}. \end{aligned} \tag{B.57}$$

From (B.54) and (B.57) and by applying the LaSalle-Yoshizawa theorem, it follows that $\boldsymbol{z}_1$, $\boldsymbol{z}_2$ and $\tilde{\boldsymbol{\theta}}$ are bounded and satisfy (B.49) under condition (B.47). From (B.28) and Lemma 1 it follows that the control input $\boldsymbol{u}$, where only quantized states are measured, also is bounded. Thus, all signals in the closed loop system are bounded. Tracking of the desired reference signal is achieved, with a bounded tracking error given in (B.49). The value of a depends on the quantization parameters, and higher values of the quantization intervals will increase a, and if there is no quantization then $a = 0$.

B.4 Experimental Results

The proposed controller was simulated using MATLAB/Simulink and tested on the Quanser Aero helicopter system, shown in Fig. B.2. This is a two-rotor laboratory equipment for flight control-based experiments. The setup has a horizontal position of the main thruster and a vertical position of the tail thruster, which resembles a helicopter with two propellers driven by two DC motors. This is a MIMO system

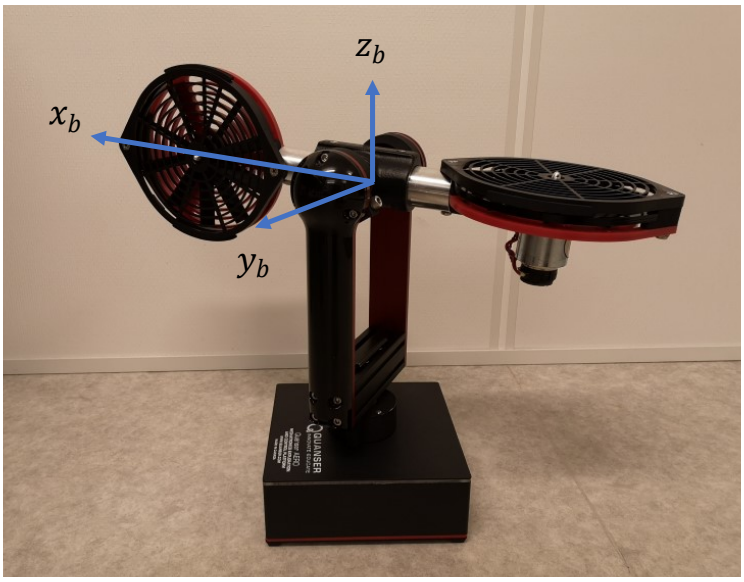

Figure B.2: Quanser Aero helicopter system with body coordinate frame.

Table B.1: Helicopter Parameters.

Symbol	Value	Units
$\boldsymbol{J}$	$\text{diag}(0.0218, 0.0217, 0.0218)$	kgm^2
m	1.075	kg
g	9.81	m/s^2
$\boldsymbol{r}_b^g$	$[0 \;\; 0 \;\; -0.0038]^\top$	m
$\boldsymbol{B}$	$\begin{bmatrix} 1 & 0 & 0 \\ 0 & 0.0011 & 0.0011 \\ 0 & -0.0014 & 0.00176 \end{bmatrix}$	Nm/V

with 2 DOF, and the helicopter can rotate around two axes where each input affects both rotational directions. The body fixed coordinate frame is visualized in Fig. B.2, and the inertial frame is coinciding with the body frame when $\boldsymbol{q} = [\pm 1 \; 0 \; 0 \; 0]^\top$. The mathematical model is described by (B.1) and (B.2), and the parameters used for simulation and experiments are shown in Table B.1. The initial states and estimated parameters were chosen as $\boldsymbol{q}(t_0) = [1 \; 0 \; 0 \; 0]^\top$, $\boldsymbol{\omega}(t_0) = [0 \; 0 \; 0]^\top$ and $\hat{\boldsymbol{\theta}}(t_0) = [0 \; 0.0070 \; 0.0095]^\top$ and the design parameters were set to $C_1 = 0.3\boldsymbol{I}$, $C_2 = 0.15\boldsymbol{I}$ and $\boldsymbol{\Gamma} = 0.02\boldsymbol{I}$. The objective was to track a sinusoidal signal where $r_d = 0$, $p_d = 40\pi/180 \sin(0.1\pi t)$, $y_d = 100\pi/180 \sin(0.05\pi t)$, given in Euler angles, and converted to a quaternion, and see how the system was affected by quantization of the states and validate the findings in Theorem 1. The quantization level for all measured states were chosen as $l = 2/2^R$, where R is number of bits transmitted in the communication. The system was first tested with continuous states, then with different values for R.

The results from the test with quantized states, where $R = 7$ are shown in Figs. B.3-B.5, showing the states $\boldsymbol{q}^Q$, $\boldsymbol{\omega}^Q$, the error in attitude and in angular velocity

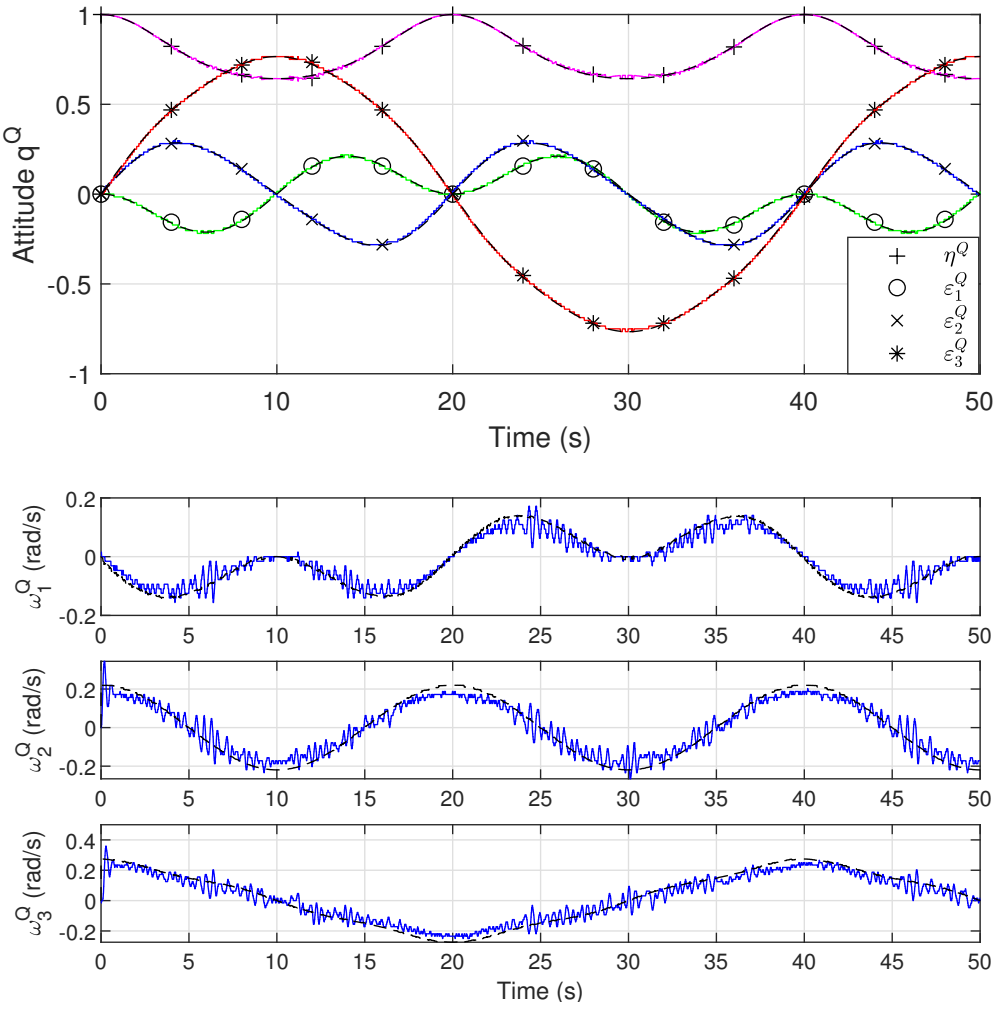

Figure B.3: The attitude $\boldsymbol{q}^Q$ and the angular velocity $\boldsymbol{\omega}^Q$ from experiment.

$\tilde{\boldsymbol{\varepsilon}}^Q$, $\boldsymbol{\omega}_e^Q$, and the input $\boldsymbol{u}(\boldsymbol{q}^Q, \boldsymbol{\omega}^Q)$, respectively. The desired states are shown with a dotted line and measured values from tests on the helicopter model are shown with a solid line. Since we only have 2 motors on the helicopter model, the control allocation matrix $\boldsymbol{B}$, was chosen so that the input $u_1 = 0$, and is not included in the plot of the input in Fig. B.5.

The total tracking error z_{track} was measured, where

$$z_{\text{track}} = \int_{t_0}^{t_f} \tilde{\boldsymbol{\varepsilon}}(\tau)^{Q,\top} \tilde{\boldsymbol{\varepsilon}}(\tau)^Q d\tau, \tag{B.58}$$

with $t_0 = 0$ and $t_f = 50$ s. The tracking errors for different values of R are shown in Table B.2. For values $R \geq 9$, the system does not show a big difference in performance compared to when using continuous signals. A lower value for R is also possible, and will require less data transmission, but with the cost of higher tracking error and also with more chattering for the input.

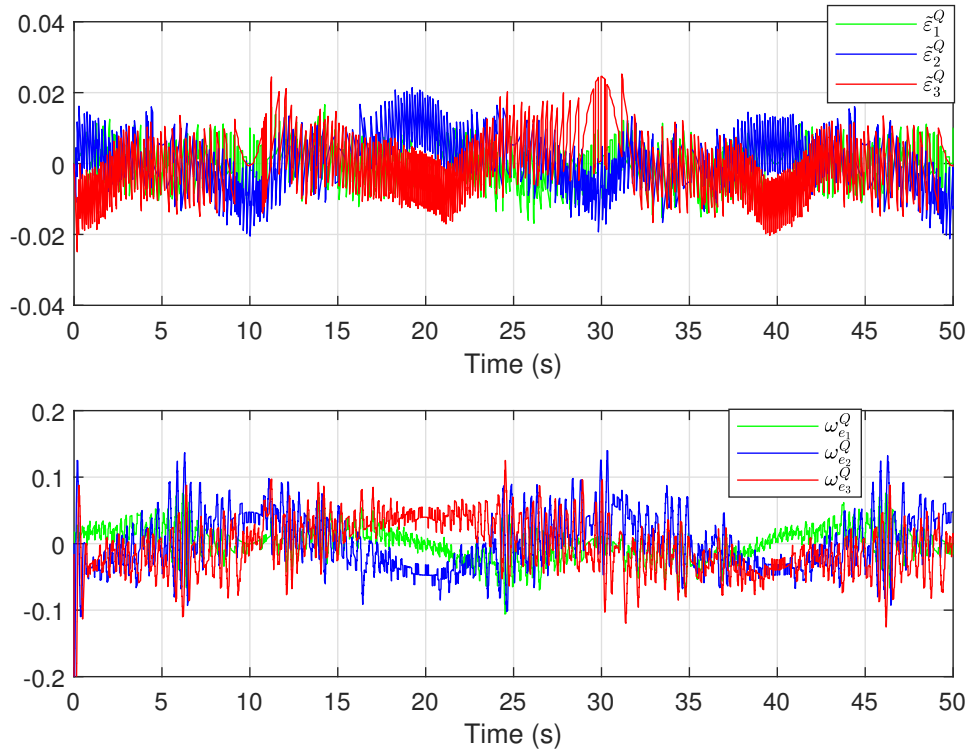

Figure B.4: The error in attitude $\tilde{\boldsymbol{\varepsilon}}^Q$ and the angular velocity error $\boldsymbol{\omega}_{\boldsymbol{e}}^Q$ from experiment.

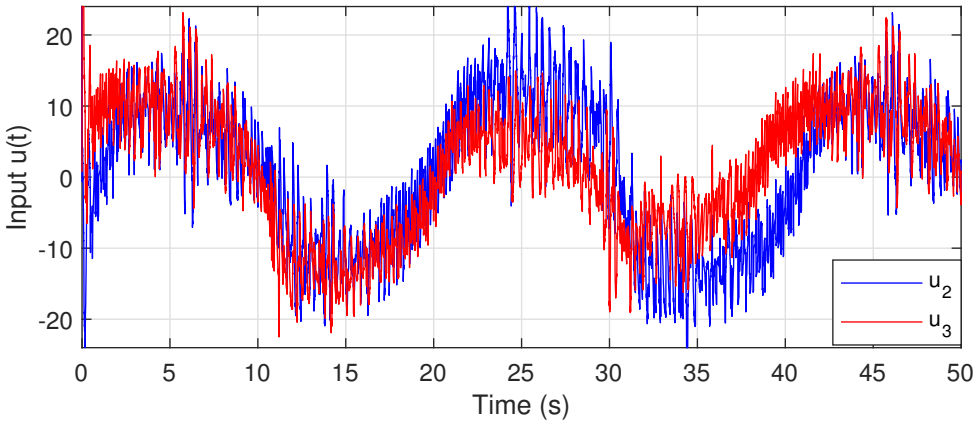

Figure B.5: The input $\boldsymbol{u}(\boldsymbol{q}^Q, \boldsymbol{\omega}^Q)$ from experiment.

Table B.2: Tracking error for different quantization levels, $l = 2/2^R$, from test on helicopter model.

$z_{\mathbf{track}}$	$\boldsymbol{\omega}^Q$				
$\boldsymbol{\varepsilon}^Q$	R	7	8	9	cont.
	7	0.0072	0.0075	0.0074	-
	8	0.0043	0.0043	0.0044	-
	9	0.0042	0.0039	0.0035	-
	cont	-	-	-	0.0035

B.5 Conclusion

In this paper, an adaptive backstepping control scheme is developed for attitude tracking using quaternions where the states are quantized. The quantizer considered satisfies a bounded condition and so the quantization error is bounded. With the use of constructed Lyapunov functions, all signals in the closed loop system are shown to be uniformly bounded and also tracking of a given reference signal is achieved. Experiments support the proof. As illustrated in the experiment, it is possible to reduce the communication burden over the network by including quantization and still have a good performance, where a suitable quantization level must be chosen. Actuators may reach their saturation level at some point, and this is a problem that can be further looked into.

References – Paper B

[1] S. Tatikonda and S. Mitter, "Control under communication constraints," *IEEE Transactions on Automatic Control*, vol. 49, no. 7, pp. 1056–1068, 2004.

[2] M. Fu and L. Xie, "The sector bound approach to quantized feedback control," *IEEE Transactions on Automatic Control*, vol. 50, no. 11, pp. 1698–1711, 2005.

[3] C. D. Persis, "Robust stabilization of nonlinear systems by quantized and ternary control," *Systems & Control Letters*, vol. 58, no. 8, pp. 602–608, 2009.

[4] T. Hayakawa, H. Ishii, and K. Tsumaru, "Adaptive quantized control for nonlinear uncertain systems," *Systems & Control Letters*, vol. 58, no. 9, pp. 625–632, 2009.

[5] H. Sun, N. Hovakimyan, and T. Basar, "$\mathcal{L}_1$ adaptive controller for uncertain nonlinear multi-input multi-output systems with input quantization," *IEEE Transactions on Automatic Control*, vol. 57, no. 3, pp. 565–578, 2012.

[6] J. Zhou, C. Wen, and G. Yang, "Adaptive backstepping stabilization of nonlinear uncertain systems with quantized input signal," in *IEEE Transactions on Automatic Control*, vol. 59, no. 2, 2014, pp. 460–464.

[7] J. Zhou, C. Wen, and W. Wang, "Adaptive control of uncertain nonlinear systems with quantized input signal," *Automatica*, vol. 95, pp. 152–162, 2018.

[8] D. Liberzon, "Hybrid feedback stabilization of systems with quantized signals," *Automatica*, vol. 39, no. 9, pp. 1543–1554, 2003.

[9] T. Liu and Z. Jiang, "Event-triggered control of nonlinear systems with state quantization," *IEEE Transactions on Automatic Control*, vol. 64, no. 2, pp. 797–803, 2019.

[10] T. Liu, Z.-P. Jiang, and D. J. Hill, "A sector bound approach to feedback control of nonlinear systems with state quantization," *Automatica*, vol. 48, no. 1, pp. 145–152, 2012.

[11] K. Liu, E. Fridman, and K. H. Johansson, "Dynamic quantization of uncertain linear networked control systems," *Automatica*, vol. 59, pp. 248–255, 2015.

[12] A. Selivanov, A. Fradkov, and D. Liberzon, "Adaptive control of passifiable linear systems with quantized measurements and bounded disturbances," *Systems and Control Letters*, vol. 88, pp. 62–67, 2016.

[13] J. Zhou, C. Wen, W. Wang, and F. Yang, "Adaptive backstepping control of nonlinear uncertain systems with quantized states," *IEEE Transactions on Automatic Control*, vol. 64, no. 11, pp. 4756–4763, 2019.

[14] R. Sun, A. Shan, C. Zhang, J. Wu, and Q. Jia, "Quantized fault-tolerant control for attitude stabilization with fixed-time disturbance observer," *Journal of Guidance, Control, and Dynamics*, vol. 44, no. 2, pp. 449–455, 2021.

[15] Y. Yan and S. Yu, "Sliding mode tracking control of autonomous underwater vehicles with the effect of quantization," *Ocean Engineering*, vol. 151, pp. 322–328, 2018.

[16] B. Huang, B. Zhou, S. Zhang, and C. Zhu, "Adaptive prescribed performance tracking control for underactuated autonomous underwater vehicles with input quantization," *Ocean Engineering*, vol. 221, 2021.

[17] M. Krstić, I. Kanellakopoulos, and P. Kokotović, *Nonlinear and Adaptive Control Design*. John Wiley & Sons, Inc., 1995.

[18] L. Xing, C. Wen, Y. Zhu, H. Su, and Z. Liu, "Output feedback control for uncertain nonlinear systems with input quantization," *Automatica*, vol. 65, pp. 191–202, 2015.

[19] Y. Li and G. Yang, "Adaptive asymptotic tracking control of uncertain nonlinear systems with input quantization and actuator faults," *Automatica*, vol. 72, pp. 177–185, 2016.

[20] S. M. Schlanbusch and J. Zhou, "Adaptive backstepping control of a 2-DOF helicopter system with uniform quantized inputs," in *IECON 2020 The 46th Annual Conference of the IEEE Industrial Electronics Society*, 2020, pp. 88–94.

[21] Y. Wang, L. He, and C. Huang, "Adaptive time-varying formation tracking control of unmanned aerial vehicles with quantized input," *ISA Transactions*, vol. 85, pp. 76–83, 2019.

[22] R. Schlanbusch, A. Loria, R. Kristiansen, and P. J. Nicklasson, "PD+ attitude control of rigid bodies with improved performance," in *49th IEEE Conference on Decision and Control*, 2010.